

Research Article

Characterization and Antiproliferative Activity of Nobiletin-Loaded Chitosan Nanoparticles

Ana G. Luque-Alcaraz,¹ Jaime Lizardi,² Francisco M. Goycoolea,³
Miguel A. Valdez,⁴ Ana L. Acosta,⁵ Simon B. Iloki-Assanga,⁵
Inocencio Higuera-Ciajara,⁶ and Waldo Argüelles-Monal¹

¹ Centro de Investigación en Alimentación y Desarrollo AC, Coordinación Regional Guaymas, Carret. al Varadero Nacional Km 6.6, 85480 Guaymas, SON, Mexico

² Centro de Investigación en Alimentación y Desarrollo AC, Coordinación Hermosillo, Carret. a la Victoria Km 0.6, 83304 Hermosillo, SON, Mexico

³ Institut für Biologie und Biotechnologie der Pflanzen, Westfälische Wilhelms-Universität-Münster, 48149 Münster, Germany

⁴ Departamento de Física, Universidad de Sonora, 83000 Hermosillo, SON, Mexico

⁵ Laboratorio de Investigación en Bioactivos y Alimentos Funcionales, Rubio Pharma y Asociados S.A. de C.V., 83210 Hermosillo, SON, Mexico

⁶ Centro de Investigación Científica de Yucatán, 97200 Mérida, YUC, Mexico

Correspondence should be addressed to Waldo Argüelles-Monal, waldo@ciad.mx

Received 6 June 2012; Revised 20 August 2012; Accepted 21 August 2012

Academic Editor: Fathallah Karimzadeh

Copyright © 2012 Ana G. Luque-Alcaraz et al. This is an open access article distributed under the Creative Commons Attribution License, which permits unrestricted use, distribution, and reproduction in any medium, provided the original work is properly cited.

Nobiletin is a polymethoxyflavonoid with a remarkable antiproliferative effect. In order to overcome its low aqueous solubility and chemical instability, the use of nanoparticles as carriers has been proposed. This study explores the possibility of binding nobiletin to chitosan nanoparticles, as well as to evaluate their antiproliferative activity. The association and loading efficiencies are 69.1% and 7.0%, respectively. The formation of an imine bond between chitosan amine groups and the carbonyl group of nobiletin, via Schiff-base, is proposed. Nobiletin-loaded chitosan nanoparticles exhibit considerable inhibition ($IC_{50} = 8 \mu\text{g/mL}$) of cancerous cells, revealing their great potential for applications in cancer chemotherapy.

1. Introduction

Flavonoids are a large class of compounds that have a common chemical structure. They occur widely in nature and most of them possess biological and pharmacological activities [1]. Due to this, flavonoids have attracted a great interest as potential therapeutic agents against a large variety of diseases [2–5].

Nobiletin (5,6,7,8,3',4' hexamethoxyflavone, Figure 1) is a citrus polymethoxylated flavone, which possesses an extensive range of pharmacological activities including antioxidant, antitumor properties and enhancement of adiponectin secretion, among others [2, 6–9]. The antiproliferative activity is one of the most widely studied pharmaceutical applications of this flavonoid. Nobiletin has been shown to be

very efficient at inhibiting invasion, migration and adhesion in four representative cell lines of brain tumour [10]. It has been also proved that nobiletin exhibits antiproliferative activity in ovarian and breast cancer cells, showing IC_{50} values between 31.9 and 16.8 μM [11]. Thus, it has been recognized that nobiletin may help prevent cervical cancer and may potentially be a useful agent for the treatment of certain malignancies [12].

Despite the fact that flavonoids possess a wide spectrum of pharmacological properties, their use is limited by its low aqueous solubility and chemical instability [13]. One approach to avoid these drawbacks is to include them into polymeric matrices, as is the case of nanoparticles. In fact, the use of polymeric nanoparticles as carriers of active pharmaceutical molecules allows to protect them from

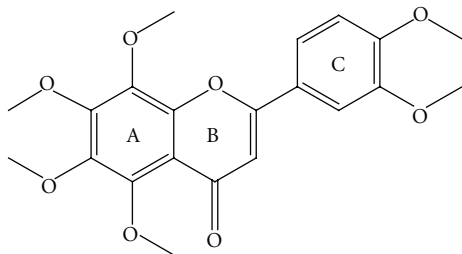


FIGURE 1: Chemical structure of nobiletin (5,6,7,8,3',4'-hexamethoxyflavone).

degradation, while delivering the bioactive molecules to the proper specific site [14]. In particular, quercetin has recently been entrapped in polymeric nanoparticles as a drug delivery system for controlled release [15].

Chitosan is a linear cationic polysaccharide, which at low pH can be dissolved behaving as a worm-like chain and composed by two kinds of $\beta(1 \rightarrow 4)$ -linked monosaccharide residues, namely, N-acetyl-D-glucosamine and D-glucosamine [16]. Chitosan is a very promising polymer for biomedical applications because of its biocompatibility, biodegradability, and low toxicity that exhibits the capacity to promote the absorption of poorly absorbed macromolecules across epithelial barriers [17–19]. Due to these properties, chitosan and its derivatives have found many pharmaceutical and biomedical applications [20].

Zhang et al. used chitosan nanoparticles to improve the bioavailability of quercetin and demonstrated that the antioxidant activity and reducing power of this flavonoid could be preserved in this type of nanosystem [21].

Thus, the objective of this investigation was to explore the possibility of binding nobiletin to chitosan nanoparticles, as well as to evaluate their antiproliferative activity. Such a strategy could be advantageous to protect nobiletin from degradation while keeping its biological activity.

2. Experimental

2.1. Materials. A commercial chitosan sample was supplied by NovaMatrix (Protasan UP B 80/20, Batch BP-0806-03). Its viscosity-average molecular weight was 1.1×10^5 , estimated at 25°C in 0.3 M acetic acid/0.2 M sodium acetate [22] and the degree of N-acetylation (DA = 0.178) was determined by ^1H NMR spectroscopy. According to the supplier, this sample has the following characteristics: Ash content 0.06%, protein content 0.13%, and endotoxins <43 EU/g. Nobiletin was acquired from Wako (Lot LTQ 5168).

All other reagents and solvents (Sigma-Aldrich) were used without further purification. Experiments were carried out with distilled water (conductivity lower than $3 \mu\text{S cm}^{-1}$).

2.2. Nanoparticle Preparation. Chitosan was dissolved in 2% acetic acid at 0.5 mg/mL to form the diffusing phase. This phase (1 or 2.5 mL) was then added to the dispersing phase (25 or 40 mL) by means of a needle positioned two centimeters above the surface at 0.86 mL/min using a peristaltic pump, under moderate magnetic stirring. This procedure

allowed nonsolvent to solvent ratios between 10 : 1 and 40 : 1. The dispersing phase was methanol, an organic solvent miscible with water in which the polymer is insoluble, the nonsolvent, optionally containing nobiletin (0.01%). The freshly formed nanoparticles were used for characterization.

2.3. Nobiletin Association Efficiency and Loading Capacity. The quantity of nobiletin entrapped in the nanoparticles was calculated by the difference between the total nobiletin incorporated in the nanoparticles formation medium and the quantity of unbound nobiletin remaining in the suspending medium. Association and loading efficiencies of the nanoparticles were determined after a simple rotatory evaporation under vacuum at 35°C and were further resuspended with water. Glycerin (2.4 μL per milliliter) was added to the suspension and nanoparticles were separated by centrifugation (10,000 $\times g$, 25°C, 40 min).

Nobiletin concentration was measured in the supernatant by HPLC on a Varian proStar 201 equipped with a Varian Microsorb-MV 100-5 C18 column and an UV-Vis proStar detector. The analysis was carried out using the following conditions: 20 μL of the supernatant was injected to the system and an eluent composed by water HPLC grade (60%) and acetonitrile (40%) at room temperature. Flow rate: 1.25 mL/min. Nobiletin was monitored by absorbance at 340 nm. Concentrations of nobiletin were quantified from integrated peak areas and calculated by interpolation from a standard curve (0–100 $\mu\text{g/mL}$).

The association and loading efficiencies of nobiletin were calculated as follows:

Association efficiency

$$= \frac{\text{Total nobiletin} - \text{Unbound nobiletin}}{\text{Total nobiletin}} \times 100,$$

Loading efficiency

$$= \frac{\text{Total nobiletin} - \text{Unbound nobiletin}}{\text{Nanoparticles weight}} \times 100.$$

(1)

2.4. Dynamic Light Scattering. Particle size and polydispersity were determined by Dynamic Light Scattering (DLS). A digital correlation system ALV-5000 (ALV-GmbH, Langeln, Germany) equipped with an Argon laser (30 mW; $\lambda_0 = 632 \text{ nm}$) was used at $25 \pm 0.1^\circ\text{C}$.

The Refractive Index was measured in a refractometer Model RE4OD (Mettler Toledo). The hydrodynamic radius, R_H , was obtained at an incident angle of 90° using the Stokes-Einstein equation:

$$D_0 = \frac{k_B T}{6\pi\eta R_H}, \quad (2)$$

where D_0 is the diffusion coefficient, k_B is the Boltzmann constant, T is the absolute temperature, and η is the viscosity of the solvent.

2.5. Atomic Force Microscopy (AFM). The experiments were conducted at room temperature in a noncontact mode using

a JEOL microscope equipped with a silicon cantilever NSC15 from MikroMasch (MikroMasch, Portland, USA). A drop of chitosan nanoparticle suspension was placed on mica and dried under atmospheric conditions before proceeding for analysis. The experiment was carried out using an Atomic Force JEOL Microscope (Scanning Probe Microscope, Model JSPM 4210, Japan).

Height and cross-sectional size measurements were carried out from AFM images with WSxM software, version 4.0, from Nanotec Electronica S.L. (Madrid, Spain) [23].

2.6. Fourier-Transform Infrared Spectroscopy (FTIR). Infrared spectra were recorded with a Nicolet Protégé 460 E.S.P. spectrometer (Madison, WI) by accumulation of 64 scans, with a resolution of 2 cm^{-1} . Samples were prepared in KBr pellets. Measurements were performed on duplicate.

2.7. Cell Lines. The following cell lines were used: RAW 264.7 (Abelson murine leukemia virus-induced tumor) and L-929 (normal subcutaneous connective tissue) purchased from the American Type Culture Collection (ATCC).

2.8. Antiproliferative Assay. Cell proliferation was determined using the standard 3-(4,5-dimethylthiazol-2-yl)-2,5-diphenyl-tetrazolium bromide (MTT) assay, which is based on the conversion of MTT to formazan crystals by mitochondrial dehydrogenases [24]. In a few words, cell suspensions ($200,000\text{ cells/mL}$) were placed in each well of a flat bottom 96-well plate and incubated at 37°C in an atmosphere of 5% CO_2 . After 18–24 hours of incubation, $50\ \mu\text{L}$ of the samples (nobiletin solution, chitosan nanoparticles and nobiletin-loaded chitosan nanoparticles) at various concentrations was added to the cells, and the incubation was continued for another 48 hours. In the last 4 hours of incubation, $10\ \mu\text{L}$ of MTT solution (5 mg/mL) was added to each well. Formed formazan crystals were dissolved with $0.05\ \text{N HCl}$ in isopropanol ($100\ \mu\text{L}$), and the absorbance was read at 570 nm on a microplate reader (Thermo Scientific Multiskan Spectrum), using a reference wavelength of 655 nm . Data were processed using SkanIt Software 2.4.2. All measurements were carried out by triplicate in three different replicates.

3. Results and Discussion

In a previous publication, we have reported the influence of the process parameters on the characteristics of chitosan nanoparticles obtained by nanoprecipitation [25]. Taking into account these results, nobiletin-loaded chitosan nanoparticles were prepared starting from a chitosan solution in aqueous acetic acid using methanol as nonsolvent, at a nonsolvent to solvent ratio 10 : 1. It is usual to consider that the bioactive substance should be dissolved with the polymer component in the solvent phase [26]. Nevertheless, in this case it was not possible, since nobiletin is sparingly soluble in aqueous media. Thus, in our protocol nobiletin was added to the nonsolvent phase.

Figure 2 shows the particle size distribution of chitosan nanoparticles and nobiletin-loaded chitosan nanoparticles,

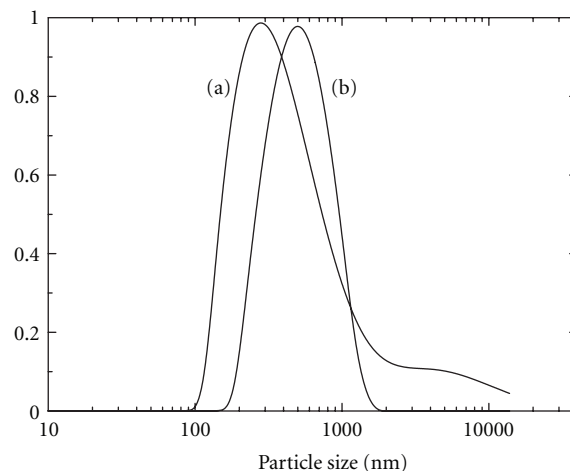
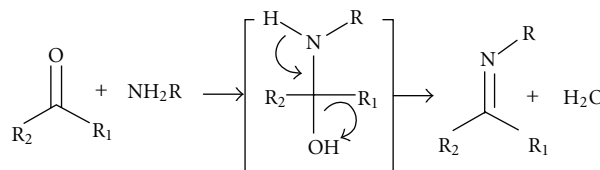


FIGURE 2: Particle sizes of (a) chitosan nanoparticles and (b) nobiletin-loaded chitosan nanoparticles as evaluated by dynamic light scattering.



SCHEME 1

giving approximate values of average size around 280 and 500 nm, respectively. It is evident that both systems present similar distribution profiles, with a monomodal pattern. Figure 3 presents the AFM image of two nobiletin-loaded chitosan nanoparticles and their line-scan profiles. The similarities in size and shape are evident. These particles are seen as round, flatted objects with diameter between 700 and 800 nm and height around 50 nm.

In order to evaluate the inclusion of nobiletin into the nanoparticulate system, the infrared spectrum was recorded. Figure 4 shows that nobiletin-loaded nanoparticles exhibit important bands at 1645 cm^{-1} (carbonyl stretching band) and a couple of signals at 1588 and 1519 cm^{-1} (C=C stretching in aromatic rings) [27]. All these bands are common with the nobiletin standard, and almost all are absent on the chitosan spectrum. Moreover, there is a band at 1626 cm^{-1} , which is associated with the probable formation of an imine bond between chitosan amine groups and the carbonyl group of nobiletin, via Schiff-base formation [28] (Scheme 1).

These results confirm the entrapment of the flavonoid within chitosan nanoparticles. Thus, it could be concluded that nobiletin became chemically bonded with chitosan. It is interesting, additionally, to underline that this reaction is reversible giving back the reactants under mild conditions, thus favoring the release of nobiletin from the nanoparticles. Quantitative analysis also confirms these results. The association and loading efficiencies were 69.1% and 7.0%, respectively. These figures are high enough and demonstrate

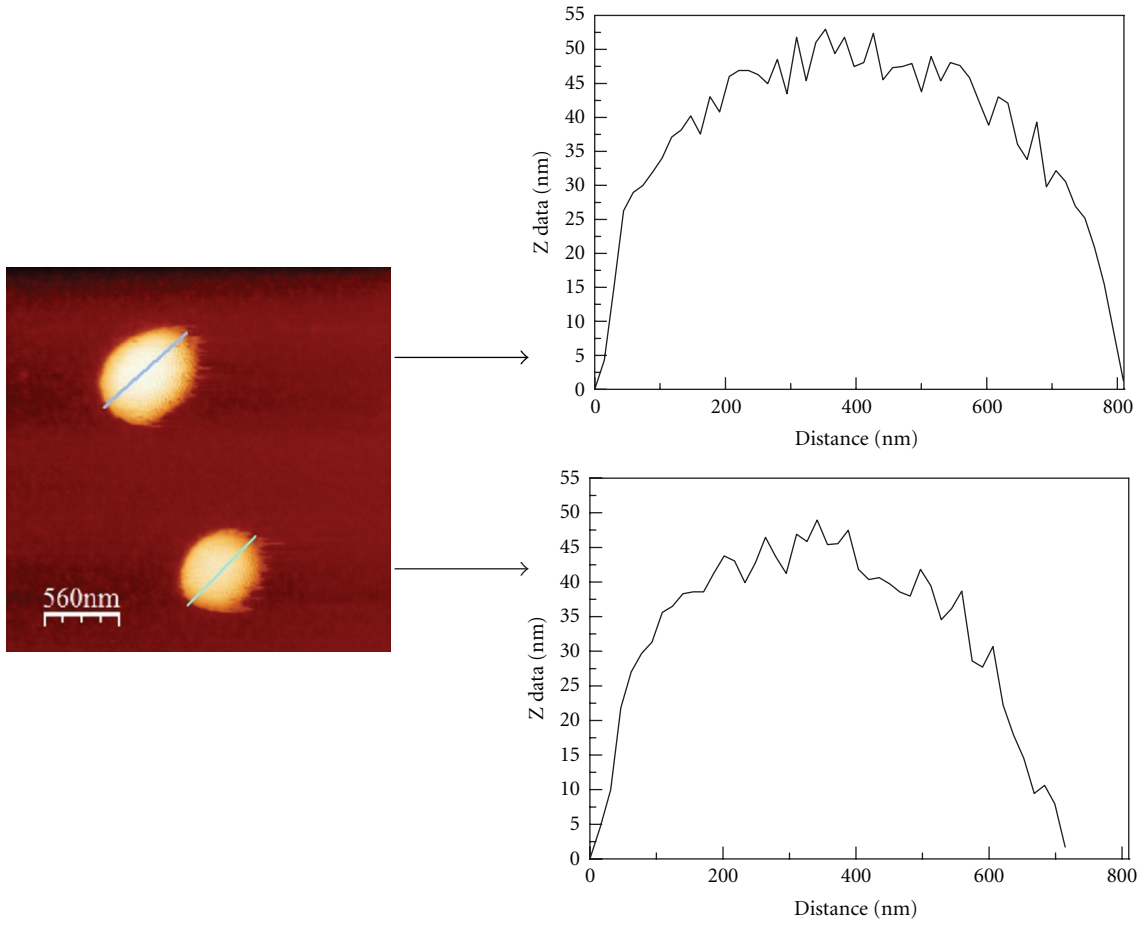


FIGURE 3: AFM image and line scan profiles of two nobiletin-loaded chitosan nanoparticles as indicated in the figure.

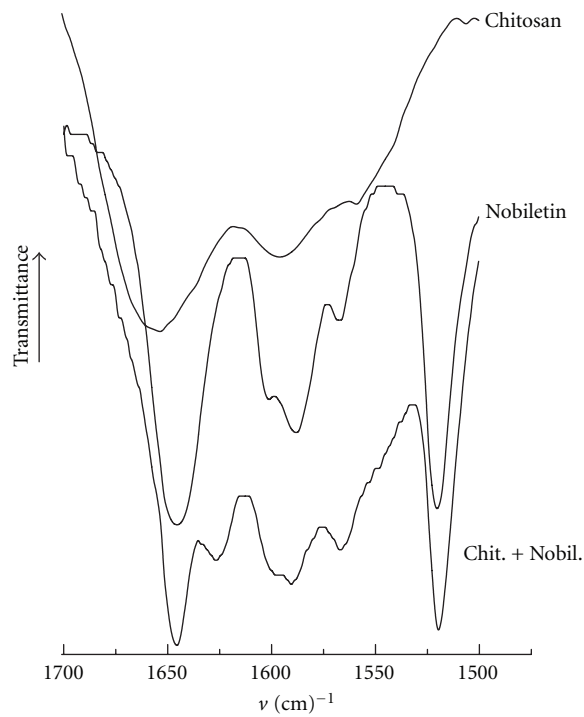


FIGURE 4: FTIR spectra of nobiletin, chitosan, and nobiletin loaded-chitosan nanoparticles as labeled.

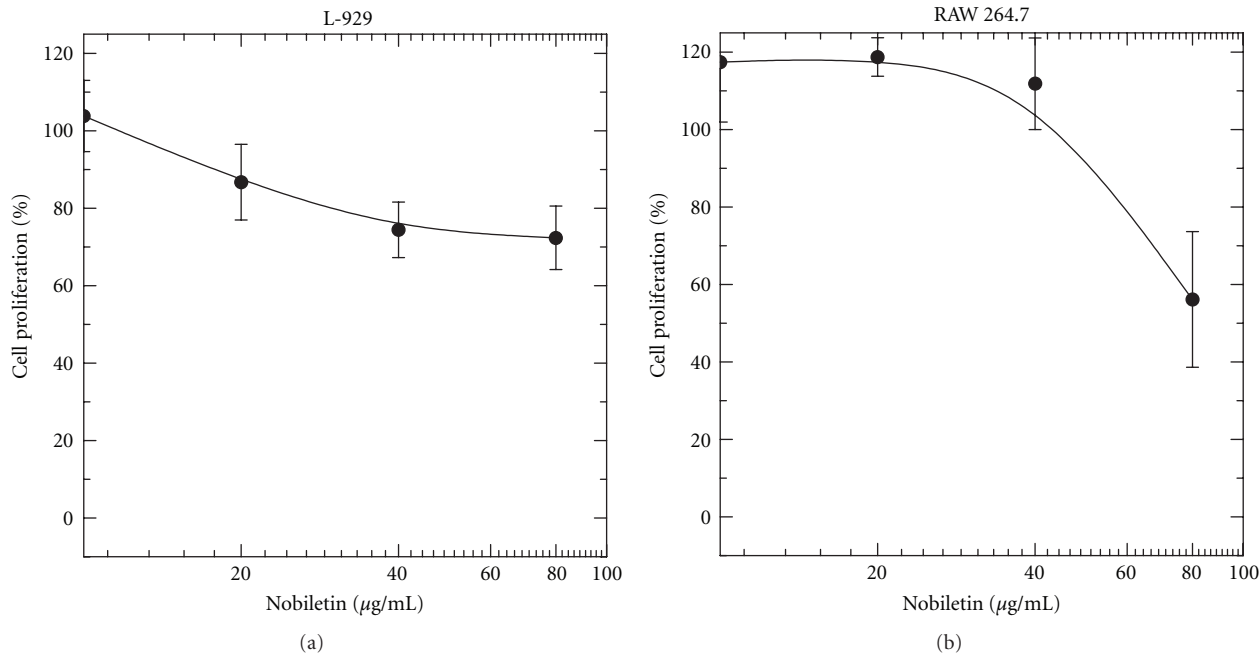


FIGURE 5: Effect of nobiletin (in solution) on cell proliferation. The type of cell line is labeled in the figure.

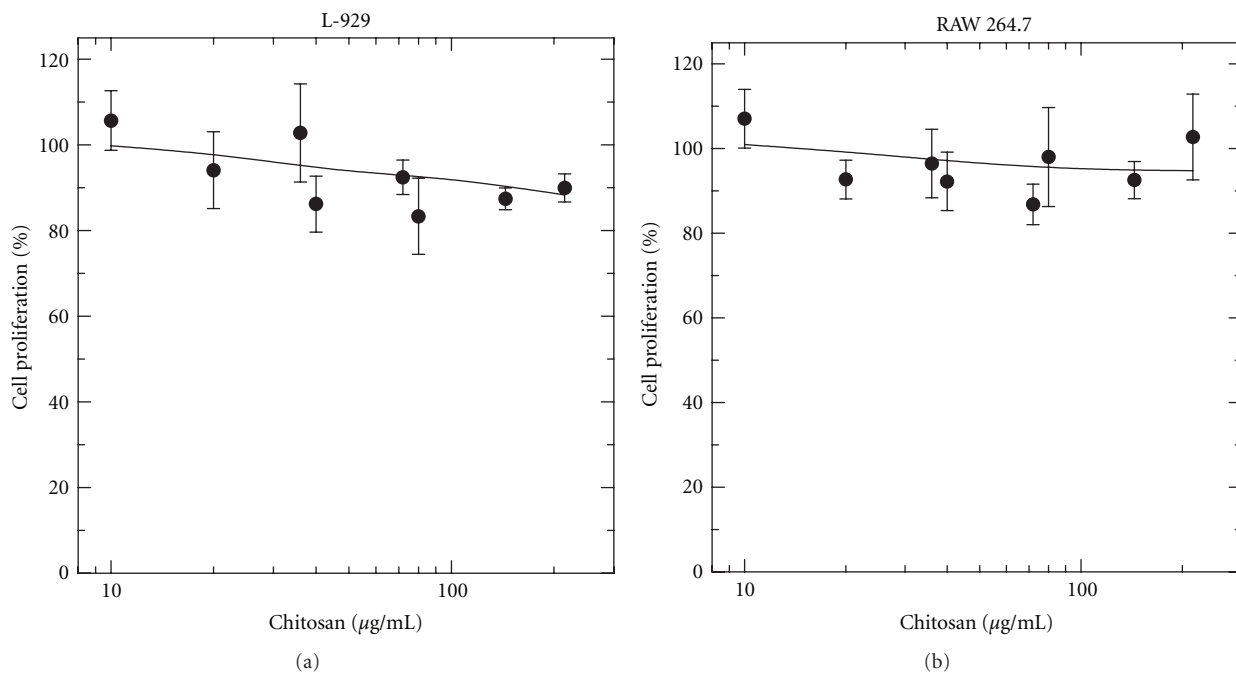


FIGURE 6: Effect of chitosan nanoparticles on cell proliferation. The type of cell line is labeled in the figure.

that the proposed process yields an adequate nanovehicle to encapsulate nobiletin.

Giving these conclusions, the antiproliferative activity of nobiletin-loaded chitosan nanoparticles was also evaluated in order to assess if the biological action had been preserved. To this end, two cell lines were chosen: one murine cancer and the other a normal subcutaneous connective tissue. Figures 5, 6, and 7 show the results obtained when both cell cultures were treated with nobiletin solution, chitosan

nanoparticles, and nobiletin-loaded chitosan nanoparticles, respectively.

On the one hand, chitosan nanoparticles do not show any antiproliferative activity over all the concentration range studied for neither cell lines (Figure 6). On the other hand, nobiletin alone does not exhibit any response against the connective tissue cells, but there is an incipient effect versus the cancer cells, particularly at concentrations above 40 µg/mL (Figure 5). Regarding nobiletin-loaded chitosan

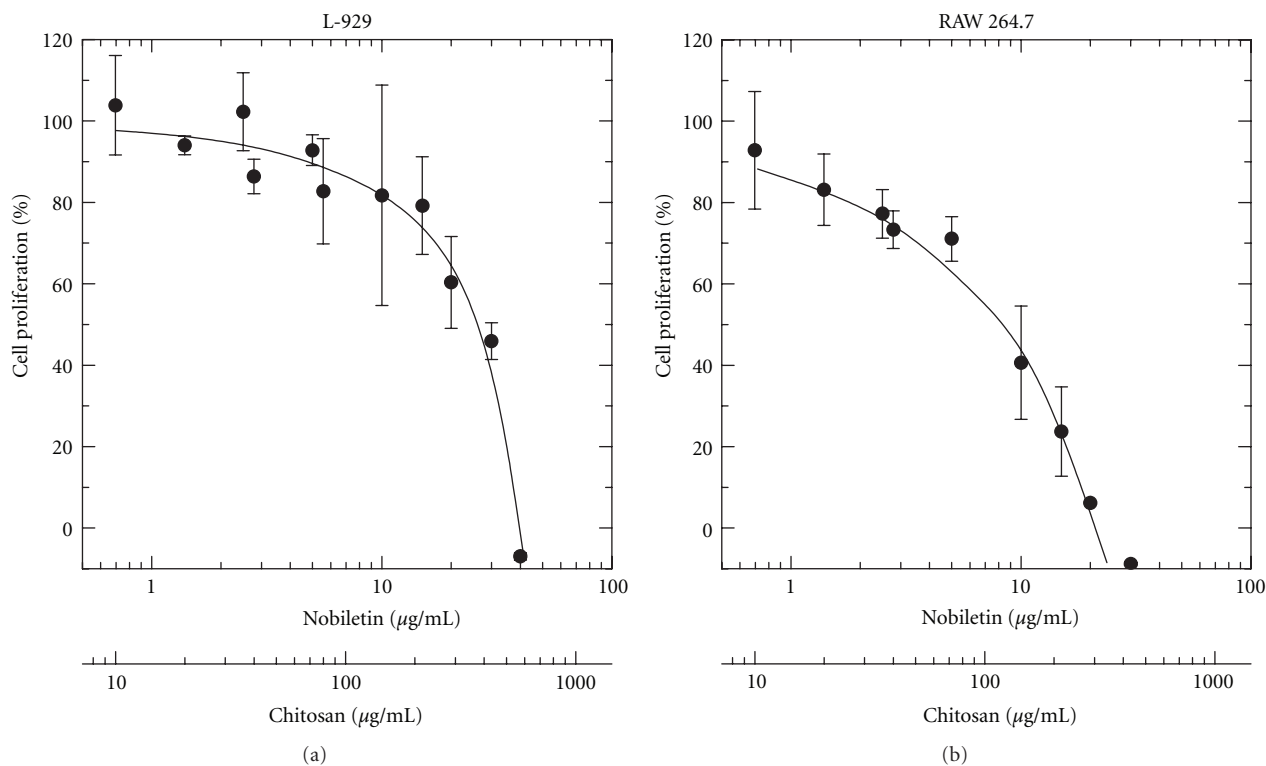


FIGURE 7: Effect of nobiletin-loaded chitosan nanoparticles on cell proliferation. The type of cell line is labeled in the figure. Cell proliferation is expressed versus nobiletin concentration and the corresponding chitosan concentration, as parallel x -axes.

TABLE 1: IC_{50} values (expressed as $\mu\text{g/mL}$) estimated from Figures 5, 6, and 7.

Sample	L-929 cells	RAW cells
Nobiletin	>80	>80
Chitosan nanoparticles	>215	>215
Nobiletin-loaded chitosan nanoparticles	26.0	8.3

nanoparticles, there is an inhibition of cellular growth in both cases (Figure 7). Nevertheless, nobiletin concentrations required to achieve this effect are lower for the murine cancer cells.

Table 1 summarizes the IC_{50} values calculated for all systems. In fact, there is a higher antiproliferative activity of nobiletin-loaded chitosan nanoparticles against the tumor culture than the connective tissue: 8.3 versus 26.0 $\mu\text{g/mL}$. The former value corresponds to a concentration of 20.1 μM , which compares satisfactorily with the IC_{50} values obtained by Du and Chen (between 31.9 and 16.8 μM) for four different cancer cell lines with nobiletin [11]. Another important effect becomes apparent when analyzing figures summarized in Table 1; nobiletin-loaded chitosan nanoparticles display a more pronounced anticancer activity than nobiletin alone. It means that the nanoencapsulation of nobiletin in chitosan particles leads to a significant enhancement of the biological effect of nobiletin. This synergistic antitumoral activity

reveals the great potential for future applications of this new nobiletin release system in cancer chemotherapy. Further investigation on this topic is required.

4. Conclusions

It was possible to encapsulate nobiletin in chitosan nanoparticles harnessed via nanoprecipitation with high association efficiency. Nobiletin-loaded chitosan nanoparticles are slightly greater than those without the flavonoid, showing a rounded-shape profile. Nobiletin becomes chemically bonded to nanoparticles via Schiff-base reaction. This nanoparticulate system exhibits improved antitumoral effect in comparison with nobiletin alone, which opens great possibilities to employ this kind of nanovehicle in chemotherapeutic techniques.

Acknowledgments

This work was financed by CONACYT-SALUD-2008-C01-87324 project, Mexico. A. G. Luque-Alcaraz thanks CONACYT for her PhD Grant. The authors would like to thank Rubio Pharma y Asociados SA de CV, to Dr. J. L. Rubio and Laboratorio de Investigación en Bioactivos y Alimentos Funcionales, for the experimental facilities to carry out this investigation. Helpful discussion with Dr. Javier Hernández (Universidad Veracruzana) is also acknowledged.

References

- [1] G. R. Beecher, "Overview of dietary flavonoids: nomenclature, occurrence and intake," *The Journal of Nutrition*, vol. 133, no. 10, pp. 3248S–3254S, 2003.
- [2] Z. Yi, Y. Yu, Y. Liang, and B. Zeng, "In vitro antioxidant and antimicrobial activities of the extract of *Pericarpium Citri Reticulatae* of a new Citrus cultivar and its main flavonoids," *LWT—Food Science and Technology*, vol. 41, no. 4, pp. 597–603, 2008.
- [3] H. Xiao, C. S. Yang, S. Li, H. Jin, C. T. Ho, and T. Patel, "Monodemethylated polymethoxyflavones from sweet orange (*Citrus sinensis*) peel inhibit growth of human lung cancer cells by apoptosis," *Molecular Nutrition & Food Research*, vol. 53, no. 3, pp. 398–406, 2009.
- [4] W. Wang and M. T. Goodman, "Antioxidant property of dietary phenolic agents in a human LDL-oxidation ex vivo model: interaction of protein binding activity," *Nutrition Research*, vol. 19, no. 2, pp. 191–202, 1999.
- [5] T. H. Wu, F. L. Yen, L. T. Lin, T. R. Tsai, C. C. Lin, and T. M. Cham, "Preparation, physicochemical characterization, and antioxidant effects of quercetin nanoparticles," *International Journal of Pharmaceutics*, vol. 346, no. 1–2, pp. 160–168, 2008.
- [6] K. Kunimasa, S. Kuranuki, N. Matsuura et al., "Identification of nobiletin, a polymethoxyflavonoid, as an enhancer of adiponectin secretion," *Bioorganic & Medicinal Chemistry Letters*, vol. 19, no. 7, pp. 2062–2064, 2009.
- [7] Y. Q. Wu, C. H. Zhou, J. Tao, and S. N. Li, "Antagonistic effects of nobiletin, a polymethoxyflavonoid, on eosinophilic airway inflammation of asthmatic rats and relevant mechanisms," *Life Sciences*, vol. 78, no. 23, pp. 2689–2696, 2006.
- [8] Y. Miyata, H. Tanaka, A. Shimada et al., "Regulation of adipocytokine secretion and adipocyte hypertrophy by polymethoxyflavonoids, nobiletin and tangeretin," *Life Sciences*, vol. 88, no. 13–14, pp. 613–618, 2011.
- [9] K. Kunimasa, M. Ikekita, M. Sato et al., "Nobiletin, a citrus polymethoxyflavonoid, suppresses multiple angiogenesis-related endothelial cell functions and angiogenesis in vivo," *Cancer Science*, vol. 101, no. 11, pp. 2462–2469, 2010.
- [10] H. K. Rooprai, A. Kandaneeratchi, S. L. Maidment et al., "Evaluation of the effects of swainsonine, captopril, tangeretin and nobiletin on the biological behaviour of brain tumour cells in vitro," *Neuropathology and Applied Neurobiology*, vol. 27, no. 1, pp. 29–39, 2001.
- [11] Q. Du and H. Chen, "The methoxyflavones in *Citrus reticulata* Blanco cv. ponkan and their antiproliferative activity against cancer cells," *Food Chemistry*, vol. 119, no. 2, pp. 567–572, 2010.
- [12] H. Kim, J. Y. Moon, A. Mosaddik, and S. K. Cho, "Induction of apoptosis in human cervical carcinoma HeLa cells by polymethoxylated flavone-rich *Citrus grandis* Osbeck (Dangyuja) leaf extract," *Food and Chemical Toxicology*, vol. 48, no. 8–9, pp. 2435–2442, 2010.
- [13] T. Pralhad and K. Rajendrakumar, "Study of freeze-dried quercetin-cyclodextrin binary systems by DSC, FT-IR, X-ray diffraction and SEM analysis," *Journal of Pharmaceutical and Biomedical Analysis*, vol. 34, no. 2, pp. 333–339, 2004.
- [14] C. S. S. R. Kumar, Ed., *Biological and Pharmaceutical Nanomaterials*, Wiley-VCH, Weinheim, Germany, 2006.
- [15] A. C. H. Barreto, V. R. Santiago, S. E. Mazzetto et al., "Magnetic nanoparticles for a new drug delivery system to control quercetin releasing for cancer chemotherapy," *Journal of Nanoparticle Research*, vol. 13, no. 12, pp. 6545–6553, 2011.
- [16] G. A. F. Roberts, *Chitin Chemistry*, The Macmillan Press, London, UK, 1st edition, 1992.
- [17] S. Hirano, H. Tsuchida, and N. Nagao, "N-acetylation in chitosan and the rate of its enzymic hydrolysis," *Biomaterials*, vol. 10, no. 8, pp. 574–576, 1989.
- [18] S. Aiba, "Studies on chitosan: 4. Lysozymic hydrolysis of partially N-acetylated chitosans," *International Journal of Biological Macromolecules*, vol. 14, no. 4, pp. 225–228, 1992.
- [19] M. N. V. R. Kumar, R. A. A. Muzzarelli, C. Muzzarelli, H. Sashiwa, and A. J. Domb, "Chitosan chemistry and pharmaceutical perspectives," *Chemical Reviews*, vol. 104, no. 12, pp. 6017–6084, 2004.
- [20] H. Sashiwa and S. I. Aiba, "Chemically modified chitin and chitosan as biomaterials," *Progress in Polymer Science*, vol. 29, no. 9, pp. 887–908, 2004.
- [21] Y. Zhang, Y. Yang, K. Tang, X. Hu, and G. Zou, "Physicochemical characterization and antioxidant activity of quercetin-loaded chitosan nanoparticles," *Journal of Applied Polymer Science*, vol. 107, no. 2, pp. 891–897, 2008.
- [22] M. Rinaudo, M. Milas, and P. le Dung, "Characterization of chitosan. Influence of ionic strength and degree of acetylation on chain expansion," *International Journal of Biological Macromolecules*, vol. 15, no. 5, pp. 281–285, 1993.
- [23] I. Horcas, R. Fernández, J. M. Gómez-Rodríguez, J. Colchero, J. Gómez-Herrero, and A. M. Baro, "WSXM: a software for scanning probe microscopy and a tool for nanotechnology," *Review of Scientific Instruments*, vol. 78, no. 1, Article ID 013705, 8 pages, 2007.
- [24] T. Mosmann, "Rapid colorimetric assay for cellular growth and survival: application to proliferation and cytotoxicity assays," *Journal of Immunological Methods*, vol. 65, no. 1–2, pp. 55–63, 1983.
- [25] A. Luque-Alcaraz, J. Lizardi, F. M. Goycoolea, M. Valdez, I. Higuera-Ciapara, and W. Argüelles-Monal, "Preparation of chitosan nanoparticles by nanoprecipitation," *Colloid and Polymer Science*. In press.
- [26] U. Bilati, E. Allémann, and E. Doelker, "Development of a nanoprecipitation method intended for the entrapment of hydrophilic drugs into nanoparticles," *European Journal of Pharmaceutical Sciences*, vol. 24, no. 1, pp. 67–75, 2005.
- [27] J. A. Manthey, "Fourier transform infrared spectroscopic analysis of the polymethoxylated flavone content of orange oil residues," *Journal of Agricultural and Food Chemistry*, vol. 54, no. 9, pp. 3215–3218, 2006.
- [28] X. Meng, L. A. Munishkina, A. L. Fink, and V. N. Uversky, "Molecular mechanisms underlying the flavonoid-induced inhibition of α -synuclein fibrillation," *Biochemistry*, vol. 48, no. 34, pp. 8206–8224, 2009.



Hindawi

Submit your manuscripts at
<http://www.hindawi.com>

